

## Article

# Visible to Mid-IR Supercontinuum Generation in Cascaded PCF-Germanate Fiber Using Femtosecond Yb-Fiber Pump

Maksim Yu. Koptev <sup>1</sup>, Alexander E. Zaprialov <sup>1</sup>, Alexey F. Kosolapov <sup>2</sup>, Alexander N. Denisov <sup>2</sup>, Maria S. Muravyeva <sup>3</sup>, Sergey L. Semjonov <sup>2</sup>, Sergey V. Muravyev <sup>1</sup> and Arkady V. Kim <sup>1,\*</sup>

<sup>1</sup> A.V. Gaponov-Grekhov Institute of Applied Physics of the Russian Academy of Sciences, 46 Ulyanov Str., 603950 Nizhny Novgorod, Russia; maksim.koptev@ipfran.ru (M.Y.K.); zaprialov12345@mail.ru (A.E.Z.); sergey-muravyev@yandex.ru (S.V.M.)

<sup>2</sup> Prokhorov General Physics Institute of the Russian Academy of Sciences, Dianov Fiber Optics Research Center, 38 Vavilov Str., 119333 Moscow, Russia; kaf@fo.gpi.ru (A.F.K.); denisov@fo.gpi.ru (A.N.D.); sls@fo.gpi.ru (S.L.S.)

<sup>3</sup> Department of Medical Biophysics, Privolzhsky Research Medical University, 10/1 Minin and Pozharsky sq., 603005 Nizhny Novgorod, Russia; masha-muravyeva@mail.ru

\* Correspondence: arkady.kim@ipfran.ru

**Abstract:** Broadband supercontinuum (SC) fiber sources covering the mid-IR range have many significant applications, largely due to their compactness, reliability, and ease of use. However, most of the existing SC fiber sources cannot boast of either high reliability or a wide bandwidth. Thus, supercontinuum sources based on silica fibers are robust, but are not capable of generating SC in the mid-IR range. Sources based on soft glasses (tellurite, chalcogenide, etc.) generate broadband SC in the mid-IR range but are not used commercially, due to the poor mechanical and chemical characteristics of such fibers. In this work, we propose a new approach consisting of cascade generation of a supercontinuum sequentially in a silica photonic crystal fiber (PCF) and a germanate fiber. Using a standard ytterbium chirped-pulse amplification (CPA) laser system for pumping, we have demonstrated a supercontinuum in the range of 450–2950 nm in PCF and germanate fiber firmly connected by a standard fusion splicing technique. Further optimization of the cascade pump will make it possible to create a compact and reliable all-fiber SC source from the visible to mid-IR range.

**Keywords:** supercontinuum generation; photonic crystal fiber; germanate fiber; femtosecond fiber laser; ytterbium-doped fiber laser



**Citation:** Koptev, M.Y.; Zaprialov, A.E.; Kosolapov, A.F.; Denisov, A.N.; Muravyeva, M.S.; Semjonov, S.L.; Muravyev, S.V.; Kim, A.V. Visible to Mid-IR Supercontinuum Generation in Cascaded PCF-Germanate Fiber Using Femtosecond Yb-Fiber Pump. *Fibers* **2023**, *11*, 72. <https://doi.org/10.3390/fib11090072>

Academic Editor: Paulo Caldas

Received: 14 July 2023

Revised: 14 August 2023

Accepted: 22 August 2023

Published: 24 August 2023



**Copyright:** © 2023 by the authors. Licensee MDPI, Basel, Switzerland. This article is an open access article distributed under the terms and conditions of the Creative Commons Attribution (CC BY) license (<https://creativecommons.org/licenses/by/4.0/>).

## 1. Introduction

Since the first experimental demonstration of supercontinuum generation in quartz glass by Alfano, R.R. and Shapiro, S.L. [1], this phenomenon has been attracting the attention of many researchers around the world. Moreover, more than 50 years later, the development of supercontinuum sources is still underway, largely due to the unique properties of this radiation and its wide range of applications. Sources of coherent supercontinuum (SC), i.e., intense lasers combined with nonlinear media for the generation of an ultra-wide band light, currently find many applications in spectroscopy [2], metrology [3], biomedicine [4], imaging [5], optical coherence tomography [6,7], and telecommunication [8]. Optical fibers are the most convenient media for supercontinuum generation, since they have high nonlinearity, long interaction lengths, and excellent output beam quality, as well as being able to ensure the ease of operation and radiation delivery. The most widely used SC fiber sources are those based on silica photonic crystal fibers (PCFs). The special design of such fibers makes it possible to optimize the group velocity dispersion (GVD) profile so that the pump pulse wavelength falls into the region of low anomalous dispersion. This leads to a wide soliton-driven nonlinear dynamic and enables the generation of a broadband supercontinuum over the entire transparency range of silica glass.

On the other hand, the possibility of low-loss splicing of such fibers with standard silica fibers [9,10] allows the creation of compact and reliable all-fiber SC sources. However, the maximum wavelength of such sources is limited by the transparency region of silica glass and does not exceed 2400 nm. Thus, Kang Kang Chen et al. [11] demonstrated supercontinuum generation in the 400–2250 nm range in a photonic crystal fiber with a core diameter of 4.4  $\mu\text{m}$  and a high (80%) pump launching efficiency. Xue Qi et al. [12] demonstrated supercontinuum in the 350–2400 nm range with an output power of 80 W in a seven-core photonic crystal fiber. To generate a supercontinuum in a longer wavelength region, tellurite, ZBLAN, and chalcogenide fibers are usually used. They have a wide range of transparency (up to 16  $\mu\text{m}$  for the chalcogenide ones) and high nonlinearity (several orders of magnitude higher than that of silica glass), which makes it possible to create on the basis of their supercontinuum sources extending further into the mid-IR. Thus, the generation of a supercontinuum in the wavelength range of 1100–2600 nm in a tellurite photonic crystal fiber pumped by femtosecond pulses at the output of an erbium fiber laser system was demonstrated in [13]. SC generation in the range of 0.6–3.3  $\mu\text{m}$  in a tellurite-tapered suspended core fiber was demonstrated in [14]; however, to achieve this result, the authors used a complicated parametric oscillator generating 200-fs pulses at a wavelength of 1730 nm. A supercontinuum with an average power of tens of watts and a spectral range reaching a wavelength of 4.3  $\mu\text{m}$  was demonstrated in ZBLAN fibers pumped with thulium fiber sources [15,16]. However, the longest wavelength SC sources were built on the basis of chalcogenide fibers [17]. They achieved a supercontinuum reaching 16  $\mu\text{m}$  of the longest wavelength; however, the zero-group velocity dispersion point of about 5  $\mu\text{m}$  makes it impossible to use fiber sources for pumping. However, several properties, including poor mechanical strength and a tendency to crystallize and absorb atmospheric moisture, significantly limit the commercial use of SC sources based on such (tellurite, ZBLAN, chalcogenide) fibers. Another limiting factor is the difficulty of launching pump radiation into such fibers, since, due to their low melting point, they cannot be spliced into standard silica fibers. The same factor applies to various gas- and liquid-filled fibers [18,19]. An alternative and promising method is to use germanate fibers for SC generation. Their nonlinearity is several times higher than that of silica fibers, and their transparency region may even exceed 3  $\mu\text{m}$  in the long-wavelength region. But their key feature is that their physical properties are similar to those of silica fibers, which makes it easy to splice such types of fiber with each other. Previously, we have experimentally demonstrated all-fiber supercontinuum sources based on germanate fibers using femtosecond erbium (SC in the range of 1–2.6  $\mu\text{m}$ ) and thulium (SC in the range of 1.9–3  $\mu\text{m}$ ) fiber lasers as pumps [20]. Moreover, a supercontinuum reaching a wavelength of 3.6  $\mu\text{m}$  was demonstrated on a short piece of a germanate fiber [21]. However, most supercontinuum fiber sources based on germanate fibers use erbium [20,22,23] or thulium [20,21,24,25] fiber lasers as pumps. Such lasers (with high peak power) are more difficult to manufacture and, as a rule, have worse output characteristics (efficiency and peak power) than the well-developed ytterbium counterparts. Moreover, thulium and erbium pumps do not allow effective supercontinuum generation in the visible range in germanate fibers. In this paper, we demonstrate a novel approach consisting of cascade generation of a supercontinuum sequentially in a silica photonic crystal fiber and a tapered germanate fiber. In this case, the silica fiber is responsible for the visible and near-IR parts of the supercontinuum, while the SC is extended to the mid-IR range in the germanate fiber. Our approach has the following two key advantages: (i) the use of efficient and well-developed ultrashort-pulse ytterbium fiber lasers as a pump, and (ii) the ability to connect all of the fibers used by the standard fusion splicing technology. All of this makes it possible to create compact and reliable all-fiber supercontinuum sources that are ready for commercial use in the ultra-wide wavelength range of 450–2950 nm. Summarizing the above, in Table 1 we present a comparison of our system with existing analogues using fiber lasers as pumps.

**Table 1.** Comparison of supercontinuum sources using fiber laser pumping.

Nonlinear Fiber [Reference]	Pump Source	SC Range
Silica PCF [11]	Yb-fiber laser	0.4–2.25 $\mu\text{m}$
Silica PCF [12]	Yb-fiber laser	0.35–2.4 $\mu\text{m}$
GeO <sub>2</sub> -doped fiber [20]	Er- and Tm-fiber lasers	1–2.6 $\mu\text{m}$ , 1.9–3 $\mu\text{m}$
GeO <sub>2</sub> -doped fiber [22]	Er-fiber laser	0.7–3.2 $\mu\text{m}$
GeO <sub>2</sub> -doped fiber [23]	Er-fiber laser	0.6–3.2 $\mu\text{m}$
GeO <sub>2</sub> -doped fiber [24]	Tm-fiber laser	1.74–3.5 $\mu\text{m}$
GeO <sub>2</sub> -doped fiber [25]	Tm-fiber laser	1.9–3 $\mu\text{m}$
ZBLAN fiber [15]	Tm-fiber laser	1.9–3.3 $\mu\text{m}$
ZBLAN fiber [16]	Tm-fiber laser	1.9–4.3 $\mu\text{m}$
Silica PCF-GeO <sub>2</sub> cascade <sup>1</sup>	Yb-fiber laser	0.45–2.95 $\mu\text{m}$

<sup>1</sup> Fibers used in this work.

## 2. Materials and Methods

To generate the supercontinuum, we used an all-fiber ytterbium CPA system as a pump source. The scheme of the experimental setup is shown in Figure 1. An ytterbium SESAM mode-locked fiber laser was used as a seed source in the system, generating chirped pulses at a wavelength of 1065 nm, with a repetition rate of 29.7 MHz. The source was made of polarization-maintaining fibers, according to the scheme, with a linear cavity and a chirped Bragg reflector, which is necessary to compensate for the group velocity dispersion of the fibers used in the cavity. The average output power was 2.5 mW, while the duration of the chirped pulse was estimated to be several picoseconds. The spectral width of the pulses at the output of the generator, measured at half maximum, was 7 nm, which indicates the possibility of compressing such pulses to femtosecond durations.

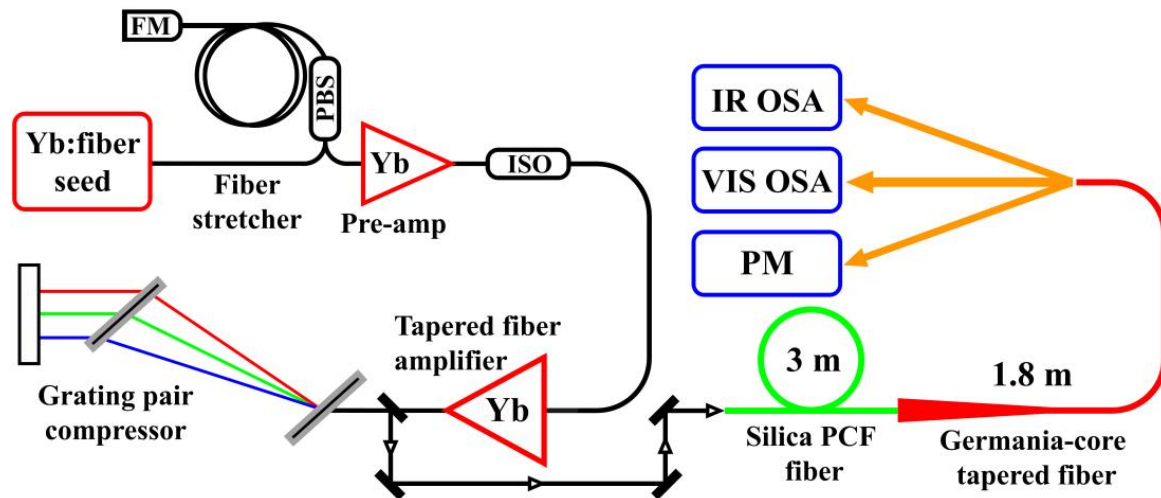


**Figure 1.** Experimental setup for broadband supercontinuum generation: FM—Faraday mirror, PBS—polarization beam splitter, ISO—Faraday isolator, IR OSA—infrared optical spectrum analyzer, VIS OSA—visible optical spectrum analyzer, PM—thermopile power meter.

To stretch the pulses, we used a piece of a special 40-m-long fiber. The group velocity dispersion and the third-order dispersion of this fiber were matched to those of the grating compressor, which ensured the most efficient pulse compression without undesirable pedestal. This became possible due to the special triple-clad design of such a fiber, which allowed precise control of its waveguide dispersion. The fiber had a normal dispersion of  $-170$  ps/nm/km and a  $D'/D$  ratio of  $3.5 \mu\text{m}^{-1}$ , whereas, the calculated value of  $D'/D$  for our grating compressor (1000 lines/mm,  $31^\circ$  angle of incidence) was  $3.3 \mu\text{m}^{-1}$ , close to that of the fiber used. The process of fabrication and the calculation of parameters for fibers of this type is described in more detail in [26]. Since the stretcher fiber was not polarization-

maintaining, we used a two-pass scheme with polarization rotation with a Faraday mirror to prevent pulse shape distortion due to depolarization. Thus, the total effective length of the stretcher was 80 m, which ensured pulse stretching to a duration of about 100 picoseconds, which was estimated as the product of the grating compressor dispersion at the best compression (14 ps/nm) and the width of the pulse spectrum (7 nm). A fiber preamplifier on a standard core-pumped ytterbium-doped PM fiber, with core/cladding diameters of 6/125  $\mu\text{m}$ , was placed after the stretcher and provided 20 mW of the average output power after the Faraday isolator.

We used a tapered ytterbium-doped active fiber as a power amplifier. Fibers of this type have an extremely high threshold of nonlinear effects while maintaining the single-mode regime of light propagation, which is necessary for efficient amplification of short pulses. We have recently shown that, in fibers of this type, it is possible to amplify chirped pulses up to a peak power of 350 kW, followed by their effective compression to 315 fs with a grating compressor [27]. In the course of the amplified signal propagation, the diameter of the fiber core adiabatically increased from 10 to 46  $\mu\text{m}$ , with the total length of the active fiber being 1.7 m. The tapered fiber was pumped in the opposite direction using a multimode laser diode with a maximum power of 60 W and a stabilized wavelength of 976 nm. The pump radiation was collimated using a plano-convex lens with a focal length of 20 mm and an antireflection coating at a wavelength of 976 nm (Thorlabs LA1074-AB-ML, Thorlabs, Newton, NJ, USA). Pumping was launched into the tapered fiber using an AR-coated best-form lens with a focal length of 40 mm (Thorlabs LBF254-040-B), which provided a magnification factor of 2 for the pump radiation spot, transferred to the end-face of the tapered fiber (from 105 to 210  $\mu\text{m}$ ). Figure 2a shows the spectrum at the output of a tapered amplifier, corresponding to an average output power of 4 W. The shape of the pulse spectrum did not undergo any changes in the process of amplification and practically coincides with the original spectral shape at the output of the master oscillator. The pulses were further compressed using a dispersion compressor based on a pair of highly efficient translucent diffraction gratings (LightSmyth LSFSG-1000-3212-94, 1000 lines/mm, LightSmyth Technologies, Eugene, OR, USA). The overall compression efficiency was 70%. The pulse duration after compression was measured using the FROG (frequency-resolved optical gating) method and amounted to 300 fs (full width at half maximum).

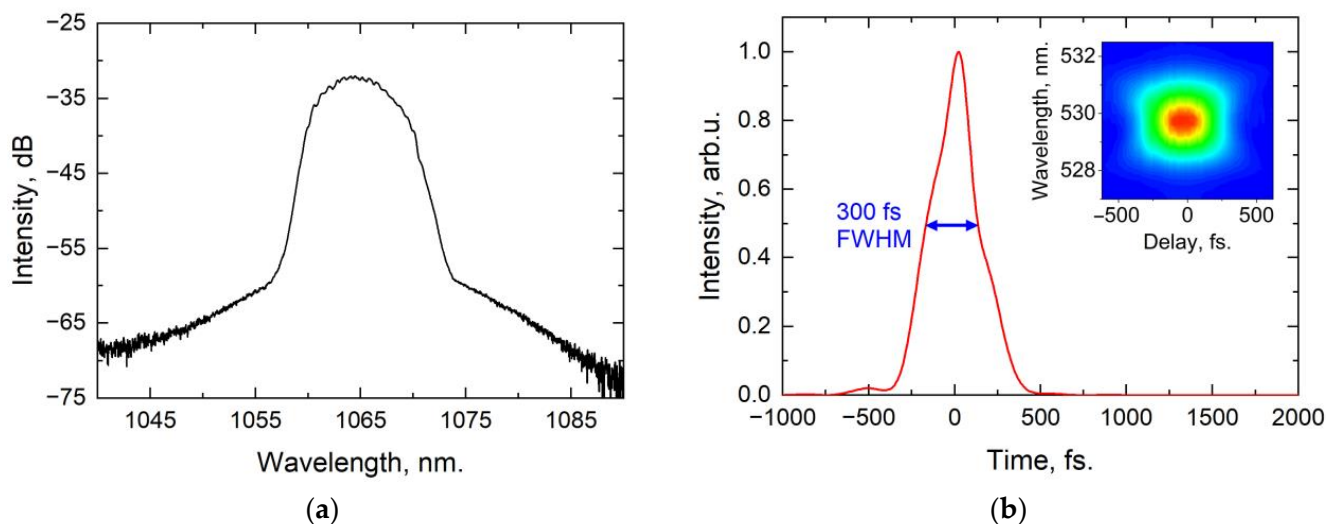


**Figure 2.** Output characteristics of the ytterbium fiber CPA laser system: (a) output spectra; (b) temporal pulse shape retrieved with FROG. Inset: Experimentally recorded FROG spectrogram of output pulses.

The temporal shape of the pulse retrieved with FROG is shown in Figure 2b. Since the tapered fiber amplifier used had a high threshold for non-linear effects, and the pulse

repetition rate was quite high (29.7 MHz), we did not observe any changes in the pulse shape or spectra up to an average output power of 10 W (14 W before the compressor), which corresponds to the compressed pulse energy of 0.3  $\mu$ J.

As the first stage of SC generation, the pulses at the output of the ytterbium CPA laser system were launched into a specially designed silica photonic crystal fiber. The fiber preform was made of the synthetic silica glass Heraeus F-300. Holes were made by drilling using tubular drills with a diamond crown. The fiber was drawn on a standard drawing installation, with excess argon pressure supplied into the holes of the preform to prevent their collapse. The fiber cladding had a standard diameter of 125  $\mu$ m, while its core had a diameter of about 4  $\mu$ m and was surrounded by 30 holes (see Figure 3a). This design allowed the zero-dispersion wavelength (ZDW) to shift to the short-wavelength region (945 nm) and provided an anomalous GVD for pump light (1065 nm). Figure 3b shows the experimentally measured dispersion of the PCF. Also, such a design ensured the operation of such a fiber in a single-mode regime in almost the entire range of silica glass transparency, which is important for practical applications and further wavelength conversion. The process of making the fibers similar to those used in this work, as well as aspects of their design, are described in more detail in Refs. [28,29].

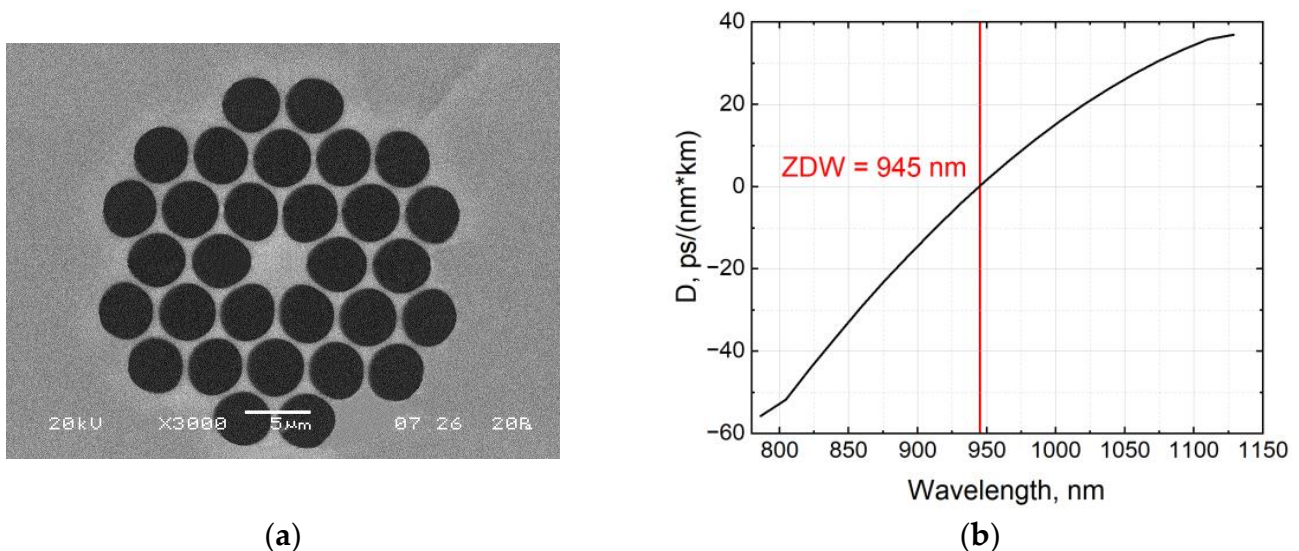


**Figure 3.** (a) Scanning electron microscope cross-sectional image of PCF core; (b) measured GVD of silica PCF.

The femtosecond pulses at the output of the dispersion compressor were launched into the PCF using an AR-coated aspherical lens with a focal length of 11 mm at a wavelength of 1064 nm (Thorlabs A220TM-B). We chose a lens with the smallest available focal length, but with a sufficient aperture for the input of collimated pump pulses. The lens provides a demagnification coefficient of 3.6 for the output of the tapered fiber, which, taking into account the diameter of its mode field of 26  $\mu$ m, allows us to estimate the diameter of the focal spot at the end of the PCF fiber to be 7  $\mu$ m. The input end of the photonic crystal fiber was carefully cleaved at a right angle with a Fujikura CT-100 (Fujikura, Koto City, Tokyo) fiber cleaver, while the quality of the cleavage, as well as the absence of damage to the core, was monitored using an optical microscope. To ensure the stability of the supercontinuum output and the ease of alignment, the input of the photonic crystal fiber was placed on a three-axis precision manual optical stage (Thorlabs NanoMax 300). The length of the PCF of 3 m was selected experimentally to provide the maximum power of the supercontinuum in the range greater than 1.7  $\mu$ m (ZDW of germania glass). To expand the supercontinuum to a longer wavelength region, a tapered germanate fiber was connected to the PCF using fusion splicing. The fiber was manufactured using a modified chemical vapor deposition technology. The fiber core contained 97 mol% germanate oxide, while its cladding was

made of standard silica glass, providing a core/cladding diameter ratio of 1/30. The total fiber length was 1.8 m. The core diameter at the input was 6  $\mu\text{m}$  and decreased adiabatically down to 3  $\mu\text{m}$ , along the fiber length. The dependence of the diameter of the core of the tapered fiber on its length and a microimage of the fiber cross section are shown in Figure 4. The fiber was tapered during the manufacturing process by changing the drawing speed. By reducing the diameter of the germanate fiber along its length, the ZDW was shifted to a longer wavelength region (due to waveguide dispersion), thereby increasing the efficiency of supercontinuum generation in the mid-IR range.

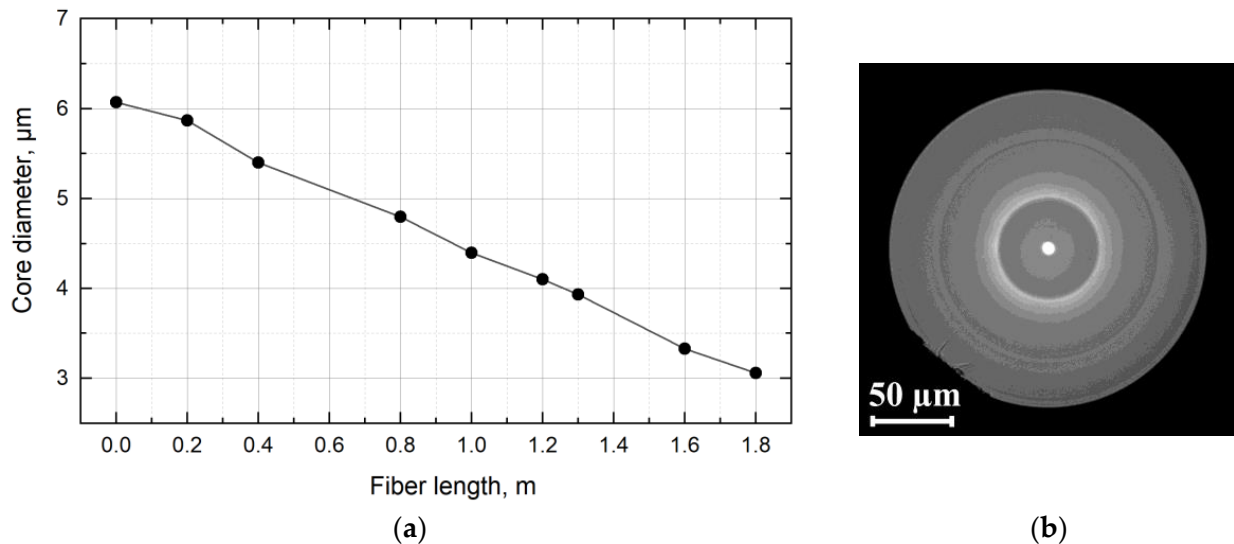


**Figure 4.** (a) Core diameter of the tapered germanate fiber versus fiber length; (b) cross-sectional image of the thick end of germanate tapered fiber, obtained with an optical microscope.

The radiation at the output of the photonic crystal fiber was launched into the germanate fiber from the thick end. The PCF and germanate fibers were spliced with a Fujikura FSM-100P+ fusion splicer in the preset mode for fibers with a cladding diameter of 80  $\mu\text{m}$ , which provided a lower arc current compared to the standard mode for splicing 125  $\mu\text{m}$  cladding fibers.

To prevent the collapse of the holes in the PCF, the welding was displaced relative to the center of the arc by 50  $\mu\text{m}$ , so that the PCF was less heated by the arc and the germanate fiber was heated more. All splicing parameters (arc current, displacement, and gap) were optimized for low splice losses, maintaining sufficient mechanical strength. The splicing loss at a weak pump signal (in the absence of strong spectrum broadening in the PCF) was measured to be 1.5 dB. The optical power was measured with a Gentec-EO UP12E (Gentec-EO, Quebec city, QC, Canada) thermopile power meter at the input of the PCF (in front of the focusing lens), at its output, and at the output of the germanate fiber. To perform spectral measurements in the mid-IR, the light at the output of the germanate fiber was collimated using a gold-plated off-axis parabolic mirror with a focal length of 2.5 cm (Thorlabs MPD119-M01). A Thorlabs OSA207C Fourier transform spectrum analyzer was used to measure the supercontinuum spectra over 1  $\mu\text{m}$ . The visible part of the spectrum was recorded with a CCD spectrum analyzer, Avantes AvaSpec-Mini4096CL (Avantes, Apeldoorn, The Netherlands), covering the range from 350 to 900 nm. Since the CCD spectrometer has a higher sensitivity than the Fourier one, the spectrum measurements in the visible range were carried out directly from the output of the germanate fiber, using a diffuser to eliminate the dependence of the output spectrum on the fiber aperture angle.

### 3. Results

Due to the optimized profile of the GVD (small anomalous dispersion at a wavelength of 1065 nm, see Figure 3a), the pumping of the PCF with femtosecond pulses led to the

generation of broadband supercontinuum, primarily because of soliton fission and Raman soliton self-frequency shift. At the same time, linear dispersive waves were efficiently generated in this fiber in the visible wavelength range. However, due to strong absorption in quartz glass, the long-wavelength part of the supercontinuum was limited to  $\sim 2.2 \mu\text{m}$  wavelength. Further wavelength conversion was carried out in a tapered germanate fiber. Such fibers are transparent up to a wavelength of  $3 \mu\text{m}$  and have previously demonstrated good conversion efficiency when using 1.5-micron pumping [30]. Figure 5 shows the experimentally measured dependences of the output power at the output of the PCF and germanate fibers on the input power measured in front of the focusing lens.

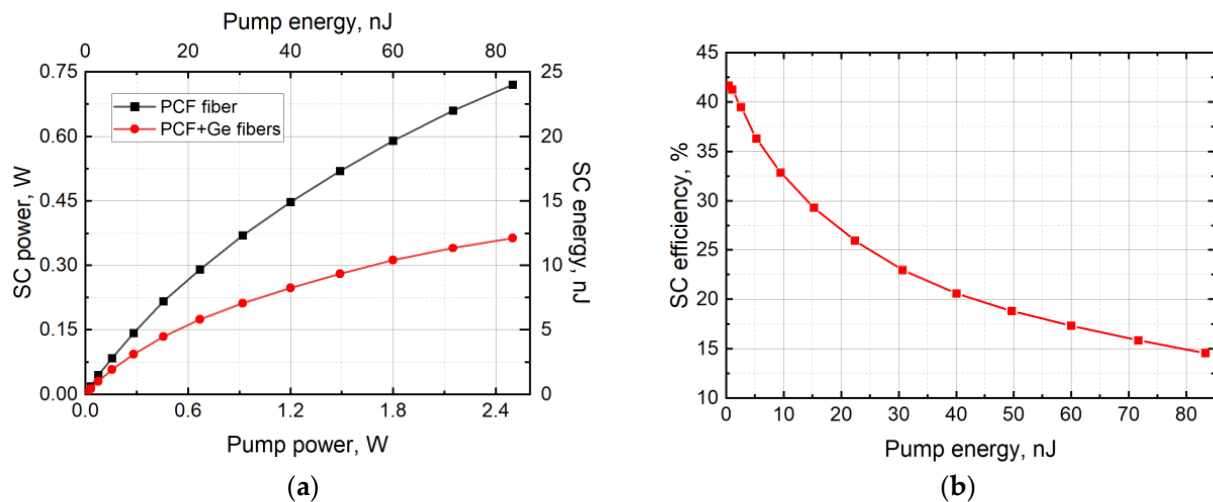


**Figure 5.** Output characteristics of supercontinuum: (a) supercontinuum power versus pump power at PCF output (black line) and cascade of photonic crystal and germanate (red line) fibers; (b) total supercontinuum generation efficiency.

At low pump energies, the nonlinear broadening of the spectrum was insignificant, and the overall efficiency of the supercontinuum generation, measured as the ratio of the power at the output of the germanate fiber to the power in front of the focusing lens (see Figure 5b), was about 40%, which was close to the value of the efficiency of pump launching into the PCF (50%). As the pump pulse energy increased, the energy efficiency of the supercontinuum generation decreased. The main reason for this was that the losses in both quartz and germanate fibers increased with increasing wavelength. Thus, along with spectrum broadening, losses increased, which led to a decrease in the energy efficiency of the supercontinuum generation. However, even at a maximum pump pulse energy of 83 nJ, the conversion efficiency was 15%, which is good considering the high efficiency of the ytterbium lasers and amplifiers used for pumping.

Figure 6 shows the output spectra of a germanate fiber, both in the visible and IR ranges.

The conversion of the spectrum to the mid-IR range began at a femtosecond pulse energy of 20 nJ, which corresponded to a peak power of 63 kW. However, the highest SC power was achieved at an energy of 83 nJ (260 kW peak power), which also corresponded to the maximum width of the generated supercontinuum: 450–2950 nm. It should be noted that, for almost any pump pulse energy, the overall dynamics of the supercontinuum are determined by both photonic crystal and germanate fibers. Therefore, even at low pulse energies of 3–10 nJ, when the long-wavelength part of the supercontinuum in the PCF fiber has not yet reached a wavelength of  $1.7 \mu\text{m}$  (ZDW of germania glass), a long-wavelength wing is observed in the spectrum up to a wavelength of  $2.5 \mu\text{m}$ , caused by the germanate fiber. The distortions in the supercontinuum spectrum near a wavelength of  $2.7 \mu\text{m}$  are associated with strong absorption lines of atmospheric moisture and are caused by a relatively long optical path when the spectrum is measured with a Fourier

spectrometer. One can see a small gap in the supercontinuum spectrum in the range of 900–1000 nm, which also coincides with the blind area of the spectrum analyzers. This gap is associated with the physical impossibility of effective wavelength conversion, both due to soliton fission and the generation of linear dispersive waves near the zero-dispersion wavelength. However, in this range, there is a small amount of radiation, and thus the supercontinuum does not have a discontinuity. At high pump pulse energies (peak power above 260 kW), an optical breakdown of the input end face of the photonic crystal fiber was observed. This problem can be partially solved by splicing an end cap at the input of the PCF fiber; however, as can be seen from Figure 6, at high peak powers, a further increase in the pulse energy does not lead to a significant broadening of the SC spectrum. Thus, we consider it to be more expedient to increase the average power of the supercontinuum, due to a higher pulse repetition rate or a transition to the picosecond regime. The instability of the supercontinuum output power during the experiment (several hours) did not exceed 5% and was largely due to the temperature drift of optomechanics, which degraded the launching alignment at the input of the PCF fiber. This instability can be significantly reduced by switching to an all-fiber mode that excludes bulk optics from the design.

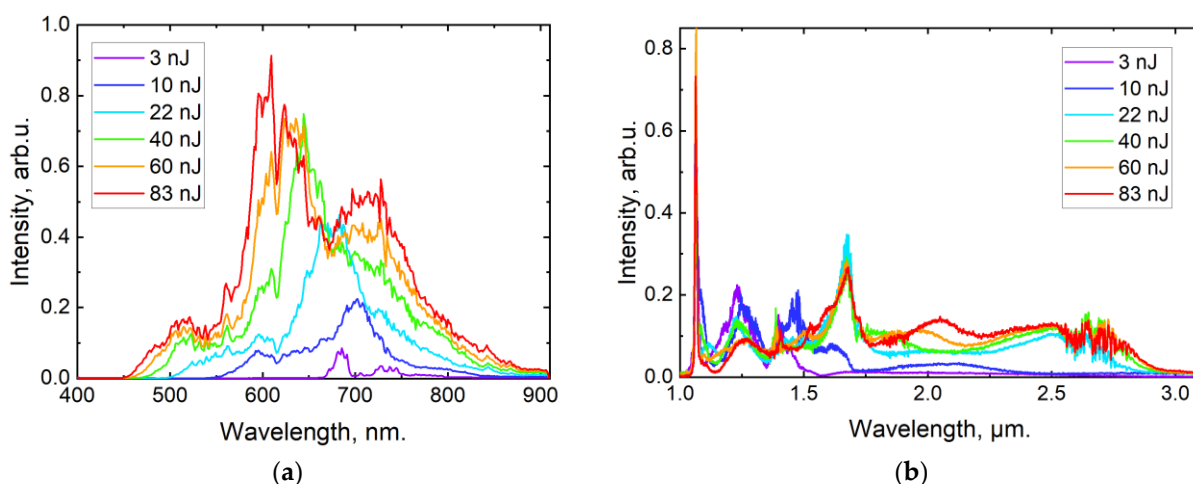


**Figure 6.** Supercontinuum spectra versus pump pulse energy in visible (a) and infrared (b) wavelength regions.

#### 4. Discussion

Currently, the most widespread sources of SC are based on optical fibers, mainly due to their simplicity, reliability, and the easy control of their optical properties, depending on the structure and manufacture material. One of the standard methods is supercontinuum generation in silica photonic crystal fibers. This method makes it possible to use the most common pulsed ytterbium lasers as pumps, while the efficiency of SC generation is ensured by a specially organized dispersion profile of the PCFs. The spectral width of the supercontinuum in this case is limited only by the transparency region of the silica fibers (~400–2400 nm). SC generation in a longer wavelength region is possible in special fibers, such as germanate, ZBLAN, tellurite, and chalcogenide fibers. However, the zero-dispersion point of such fibers is also located in the long-wavelength region far beyond 1.5  $\mu\text{m}$  and cannot be effectively shifted to the one-micron range, which impedes the use of ytterbium lasers as pumps.

The main idea and result of this work is that SC sources based on silica PCFs can generate high-power radiation in the long-wavelength region (1.8  $\mu\text{m}$  and beyond), therefore, it can be used for further conversion to the mid-IR range in suitable fibers. We focused on germanate fibers for further wavelength conversion, as they have properties closest to silica and can be easily spliced to it. Standard optical fibers, such as SMF-28, are doped with germanate oxide to increase the refractive index of the core, but they do not contain more than a percent of  $\text{GeO}_2$  in the core. With an increase in the percentage of germanate

oxide, the transparency region of the optical fibers expands, and its wavelength can reach more than 3  $\mu\text{m}$ . Because of the rather large zero-dispersion wavelength (1.7  $\mu\text{m}$ ), a typical approach to supercontinuum generation in germanate fibers is pumping with erbium or thulium fiber lasers. With the use of our approach, efficient supercontinuum generation can be achieved using ytterbium pump lasers with a simple design. In this work, we have shown the cascaded generation of SC using a femtosecond ytterbium laser. Its drawback, however, is that its grating compressor contains some bulk elements. In the future, we plan to optimize the laser design by switching to the picosecond mode. This will eliminate any bulky elements and create a compact and reliable supercontinuum source from the visible to the mid-IR range in an all-fiber design.

## 5. Conclusions

We have demonstrated broadband supercontinuum generation in the visible to mid-IR range. The advantage of our approach is the use of a cascade of silica PCFs and tapered germanate fibers. Such a structure makes it possible to use conventional ytterbium pulsed-fiber laser systems as a pump source, which are highly efficient and easy to manufacture in comparison with erbium and thulium analogs. Even though the long-wavelength limit of the supercontinuum is 3  $\mu\text{m}$  (which is less than that which can be achieved in ZBLAN, tellurite, or chalcogenide fibers), the silica PCF and the germanate fiber are spliced on a commercial fusion splicer, which makes our system robust, easy, and convenient in operation. However, the pumping system used in our work is redundant for the fibers under study. Therefore, at a pulse energy of about 90 nJ, which, considering the pulse duration, corresponds to a peak power of 260 kW, the instability of the supercontinuum parameters was observed, and at even higher energies, the optical breakdown of the end face of the silica PCF occurred. We believe that an increase in the efficiency of supercontinuum generation, as well as an increase in its output power, is possible with a transition to a picosecond pump pulse duration. This approach will also make it possible to abandon the cumbersome CPA scheme and use pulses directly amplified after the master oscillator and launched into the PCF by fusion splicing. Thus, by further optimizing the design, a compact and reliable all-fiber system generating radiation in the visible to mid-IR range can be created.

**Author Contributions:** Conceptualization, S.L.S. and A.V.K.; software, A.E.Z.; validation, M.Y.K., A.E.Z. and A.V.K.; formal analysis, M.S.M.; investigation, M.Y.K. and A.E.Z.; resources, A.F.K., A.N.D., S.L.S. and A.V.K.; data curation, A.F.K. and S.V.M.; writing—original draft preparation, M.Y.K.; writing—review and editing, A.V.K.; visualization, S.V.M.; supervision, A.V.K.; project administration, A.V.K.; funding acquisition, S.L.S. and A.V.K. All authors have read and agreed to the published version of the manuscript.

**Funding:** This research was supported by the Center of Excellence «Center of Photonics» funded by the Ministry of Science and Higher Education of the Russian Federation, contract No. 075-15-2022-316.

**Data Availability Statement:** Data underlying the results presented in this paper are not publicly available at this time but may be obtained from the authors upon reasonable request.

**Conflicts of Interest:** The authors declare no conflict of interest.

## References

1. Alfano, R.R.; Shapiro, S.L. Emission in the Region 4000 to 7000 Å Via Four-Photon Coupling in Glass. *Phys. Rev. Lett.* **1970**, *24*, 584–587. [[CrossRef](#)]
2. Holzwarth, R.; Udem, T.; Hänsch, T.W.; Knight, J.C.; Wadsworth, W.J.; Russell, P.S.J. Optical Frequency Synthesizer for Precision Spectroscopy. *Phys. Rev. Lett.* **2000**, *85*, 2264–2267. [[CrossRef](#)] [[PubMed](#)]
3. Schliesser, A.; Picqué, N.; Hänsch, T.W. Mid-Infrared Frequency Combs. *Nat. Photon* **2012**, *6*, 440–449. [[CrossRef](#)]
4. Tu, H.; Boppart, S.A. Coherent Fiber Supercontinuum for Biophotonics: Coherent Fiber Supercontinuum for Biophotonics. *Laser Photonics Rev.* **2013**, *7*, 628–645. [[CrossRef](#)]
5. Liu, S.; Liu, W.; Niu, H. Supercontinuum Generation with Photonic Crystal Fibers and Its Application in Nano-Imaging. In *Photonic Crystals*; Bananej, A., Ed.; InTech: Houston, TX, USA, 2015; ISBN 978-953-51-2121-3.
6. Marks, D.L.; Oldenburg, A.L.; Reynolds, J.J.; Boppart, S.A. Study of an Ultrahigh-Numerical-Aperture Fiber Continuum Generation Source for Optical Coherence Tomography. *Opt. Lett.* **2002**, *27*, 2010. [[CrossRef](#)]

7. Sharma, U.; Chang, E.W.; Yun, S.H. Long-Wavelength Optical Coherence Tomography at 17 Mm for Enhanced Imaging Depth. *Opt. Express* **2008**, *16*, 19712. [[CrossRef](#)]
8. Ohara, T.; Takara, H.; Yamamoto, T.; Masuda, H.; Morioka, T.; Abe, M.; Takahashi, H. Over-1000-Channel Ultradense WDM Transmission with Supercontinuum Multicarrier Source. *J. Light. Technol.* **2006**, *24*, 2311–2317. [[CrossRef](#)]
9. Xiao, L.; Demokan, M.S.; Jin, W.; Wang, Y.; Zhao, C.-L. Fusion Splicing Photonic Crystal Fibers and Conventional Single-Mode Fibers: Microhole Collapse Effect. *J. Light. Technol.* **2007**, *25*, 3563–3574. [[CrossRef](#)]
10. Xiao, L.; Jin, W.; Demokan, M.S. Fusion Splicing Small-Core Photonic Crystal Fibers and Single-Mode Fibers by Repeated Arc Discharges. *Opt. Lett.* **2007**, *32*, 115. [[CrossRef](#)]
11. Chen, K.K.; Alam, S.; Price, J.H.V.; Hayes, J.R.; Lin, D.; Malinowski, A.; Codemard, C.; Ghosh, D.; Pal, M.; Bhadra, S.K.; et al. Picosecond Fiber MOPA Pumped Supercontinuum Source with 39 W Output Power. *Opt. Express* **2010**, *18*, 5426. [[CrossRef](#)]
12. Qi, X.; Chen, S.; Li, Z.; Liu, T.; Ou, Y.; Wang, N.; Hou, J. High-Power Visible-Enhanced All-Fiber Supercontinuum Generation in a Seven-Core Photonic Crystal Fiber Pumped at 1016 Nm. *Opt. Lett.* **2018**, *43*, 1019. [[CrossRef](#)] [[PubMed](#)]
13. Klimczak, M.; Michalik, D.; Stepniewski, G.; Karpate, T.; Cimek, J.; Forestier, X.; Kasztelanic, R.; Pysz, D.; Stepień, R.; Buczyński, R. Coherent Supercontinuum Generation in Tellurite Glass Regular Lattice Photonic Crystal Fibers. *J. Opt. Soc. Am. B* **2019**, *36*, A112. [[CrossRef](#)]
14. Picot-Clemente, J.; Strutyński, C.; Amrani, F.; Désévéday, F.; Jules, J.-C.; Gadret, G.; Deng, D.; Cheng, T.; Nagasaka, K.; Ohishi, Y.; et al. Enhanced Supercontinuum Generation in Tapered Tellurite Suspended Core Fiber. *Opt. Commun.* **2015**, *354*, 374–379. [[CrossRef](#)]
15. Yang, L.; Li, Y.; Zhang, B.; Wu, T.; Zhao, Y.; Hou, J. 30-W Supercontinuum Generation Based on ZBLAN Fiber in an All-Fiber Configuration. *Photon. Res.* **2019**, *7*, 1061. [[CrossRef](#)]
16. Yang, L.; Zhang, B.; He, X.; Deng, K.; Liu, S.; Hou, J. 20.6 W Mid-Infrared Supercontinuum Generation in ZBLAN Fiber With Spectrum of 1.9–4.3 Mm. *J. Light. Technol.* **2020**, *38*, 5122–5127. [[CrossRef](#)]
17. Dai, S.; Wang, Y.; Peng, X.; Zhang, P.; Wang, X.; Xu, Y. A Review of Mid-Infrared Supercontinuum Generation in Chalcogenide Glass Fibers. *Appl. Sci.* **2018**, *8*, 707. [[CrossRef](#)]
18. Adamu, A.I.; Habib, M.S.; Petersen, C.R.; Lopez, J.E.A.; Zhou, B.; Schülzgen, A.; Bache, M.; Amezcua-Correa, R.; Bang, O.; Markos, C. Deep-UV to Mid-IR Supercontinuum Generation Driven by Mid-IR Ultrashort Pulses in a Gas-Filled Hollow-Core Fiber. *Sci. Rep.* **2019**, *9*, 4446. [[CrossRef](#)]
19. Le, H.V.; Hoang, V.T.; Nguyen, H.T.; Long, V.C.; Buczynski, R.; Kasztelanic, R. Supercontinuum Generation in Photonic Crystal Fibers Infiltrated with Tetrachloroethylene. *Opt. Quant. Electron.* **2021**, *53*, 187. [[CrossRef](#)]
20. Anashkina, E.A.; Andrianov, A.V.; Koptev, M.Y.; Muravyev, S.V.; Kim, A.V. Towards Mid-Infrared Supercontinuum Generation with Germano-Silicate Fibers. *IEEE J. Select. Top. Quantum Electron.* **2014**, *20*, 643–650. [[CrossRef](#)]
21. Yin, K.; Zhang, B.; Yao, J.; Yang, L.; Liu, G.; Hou, J. 19–36 Mm Supercontinuum Generation in a Very Short Highly Nonlinear Germania Fiber with a High Mid-Infrared Power Ratio. *Opt. Lett.* **2016**, *41*, 5067. [[CrossRef](#)]
22. Jain, D.; Sidharthan, R.; Moselund, P.M.; Yoo, S.; Ho, D.; Bang, O. Record Power, Ultra-Broadband Supercontinuum Source Based on Highly GeO<sub>2</sub> Doped Silica Fiber. *Opt. Express* **2016**, *24*, 26667. [[CrossRef](#)]
23. Yang, L.; Zhang, B.; Yin, K.; Yao, J.; Liu, G.; Hou, J. 06–32 Mm Supercontinuum Generation in a Step-Index Germania-Core Fiber Using a 44 KW Peak-Power Pump Laser. *Opt. Express* **2016**, *24*, 12600. [[CrossRef](#)] [[PubMed](#)]
24. Wang, X.; Yao, C.; Li, P.; Wu, Y.; Yang, L.; Ren, G.; Wang, C. All-Fiber High-Power Supercontinuum Laser Source over 3.5 Mm Based on a Germania-Core Fiber. *Opt. Lett.* **2021**, *46*, 3103. [[CrossRef](#)] [[PubMed](#)]
25. Zhang, M.; Kelleher, E.J.R.; Runcorn, T.H.; Mashinsky, V.M.; Medvedkov, O.I.; Dianov, E.M.; Popa, D.; Milana, S.; Hasan, T.; Sun, Z.; et al. Mid-Infrared Raman-Soliton Continuum Pumped by a Nanotube-Mode-Locked Sub-Picosecond Tm-Doped MOPFA. *Opt. Express* **2013**, *21*, 23261. [[CrossRef](#)]
26. Bobkov, K.K.; Levchenko, A.E.; Salganskii, M.Y.; Ganin, D.V.; Lyashedko, A.D.; Khudyakov, D.V.; Likhachev, M.E. Triple-Clad Optical Fibre for Pulse Stretching. *Quantum Electron.* **2021**, *51*, 894–900. [[CrossRef](#)]
27. Bobkov, K.; Andrianov, A.; Koptev, M.; Muravyev, S.; Levchenko, A.; Velmiskin, V.; Aleshkina, S.; Semjonov, S.; Lipatov, D.; Guryanov, A.; et al. Sub-MW Peak Power Diffraction-Limited Chirped-Pulse Monolithic Yb-Doped Tapered Fiber Amplifier. *Opt. Express* **2017**, *25*, 26958. [[CrossRef](#)]
28. Kosolapov, A.F.; Semjonov, S.L.; Denisov, A.N. Mechanical Properties of Microstructured High-Purity Silica Fibers. *Inorg. Mater.* **2007**, *43*, 310–314. [[CrossRef](#)]
29. Denisov, A.N.; Semjonov, S.L. Microstructured Optical Fibres with a Wide Single-Mode Range. *Quantum Electron.* **2021**, *51*, 240–247. [[CrossRef](#)]
30. Muraviev, S.V.; Dorofeev, V.V.; Motorin, S.E.; Koptev, M.Y.; Kim, A.V. Broadband Gain Performance in the Mid-IR Using Supercontinuum: 2.7 Mm Gain in High-Purity Er<sup>3+</sup> Doped Tungsten Tellurite Glass Fibers. *Appl. Opt.* **2022**, *61*, 9701. [[CrossRef](#)]

**Disclaimer/Publisher’s Note:** The statements, opinions and data contained in all publications are solely those of the individual author(s) and contributor(s) and not of MDPI and/or the editor(s). MDPI and/or the editor(s) disclaim responsibility for any injury to people or property resulting from any ideas, methods, instructions or products referred to in the content.